JGR Planets

RESEARCH ARTICLE
10.1029/2021JE006873

Formation of Ejecta and Dust Pond Deposits on Asteroid Vesta

R. Parekh[1,2], K. A. Otto[1], K. D. Matz[1], R. Jaumann[2], K. Krohn[1], T. Roatsch[1], E. Kersten[1], S. Elgner[1], C. T. Russell[3], and C. A. Raymond[4]

[1]DLR Institute of Planetary Research, Berlin, Germany, [2]Freie University of Berlin, Institute of Geological Science, Berlin, Germany, [3]University of California, Los Angeles, CA, USA, [4]Jet Propulsion Laboratory, Pasadena, CA, USA

Key Points:

- We identified ejecta and dust pond crater candidates on Vesta within 0°–30°N/S
- Ejecta ponds are smooth deposits and located within the ejecta melt of large craters
- Dust ponds are produced via local-scale seismic shaking and/or volatile fluidization

Correspondence to:
R. Parekh,
rutu.parekh@dlr.de

Citation:
Parekh, R., Otto, K. A., Matz, K. D., Jaumann, R., Krohn, K., Roatsch, T., et al. (2021). Formation of ejecta and dust pond deposits on asteroid Vesta. *Journal of Geophysical Research: Planets*, *126*, e2021JE006873. https://doi.org/10.1029/2021JE006873

Received 28 FEB 2021
Accepted 29 OCT 2021

Author Contributions:
Data curation: K. D. Matz, T. Roatsch
Funding acquisition: K. A. Otto
Resources: C. A. Raymond
Supervision: K. A. Otto, R. Jaumann
Writing – review & editing: K. A. Otto, R. Jaumann, K. Krohn, E. Kersten, C. T. Russell

Abstract Dust and melt ponds have been studied on planetary bodies including Eros, Itokawa, and the Moon. However, depending on the nature of the regolith material properties and the location of the planetary body, the formation mechanism of the ponded features varies. On Eros and Itokawa, ponded features are formed from dry regolith materials whereas on the Moon similar features are thought to be produced by ejecta melt. On the surface of Vesta, we have identified type 1, ejecta ponds, and type 2, dust ponds. On Vesta type 1 pond are located in the vicinity of ejecta melt of large impact craters. The material is uniformly distributed across the crater floor producing smooth pond surfaces which have a constant slope and shallow depth. The hosting crater of melt-like ponds has a low raised rim and is located on relatively low elevated regions. Whereas, the type 2 ponds on Vesta reveal an undulating surface that is frequently displaced from the crater center or extends toward the crater wall with an abruptly changing slope. We suggested that for the production of the type 2 ponds, localized seismic diffusion and volatile-induced fluidization may be responsible for Vesta. Due to Vesta's large size (in comparison to Eros and Itokawa), the surface may have experienced local-scale rare high-amplitude seismic diffusion which was sufficient to drift fine material. Similarly, short-lived volatile activities were capable to transfer dusty material on to the surface. Segregation and smoothing of transferred material lack further surface activities, hindering the formation of smooth morphology.

Plain Language Summary Ponded landforms are relatively smooth and featureless deposits and are commonly present on dry planetary bodies. The dry regolith of Eros, Itokawa, and the Moon provides ideal conditions for the formation of ponded deposits. They are produced either from the fine-grained regolith substances or impact crater ejecta melt material. Typically, ponded deposits are distributed homogenously and produce a flat leveled deposit surface. However, due to lack of segregation mechanisms they do not always have an entirely flat topography. The production of ponded deposits relies on geological events that include regolith migration and various mechanisms have been proposed for their formation. In our study, we identify ponded deposits on the surface of Vesta and hypothesize that rare high-amplitude seismic diffusivity and short-lived volatile outgassing were responsible for the material migration and in turn for the production of ponded deposits.

1. Introduction

Ponded deposits widely receive attention due to their unusual characteristics on asteroid Eros as revealed by the NEAR Shoemaker mission (Robinson et al., 2001, 2002; Sears et al., 2015). Usually, ponded features are identified within craters. However, there are also a few examples in which ponded features are observed in moderately large regions (Miyamoto, 2014) of a planetary body, for example, the Sagamihara and Muses-Sea regions (Fujiwara et al., 2006; Saito et al., 2006) on asteroid Itokawa. Due to their smooth appearance, they are called "ponds." Typically, ponded regions consist of a smooth layer of fine-grained material (less than cm size) (Robinson et al., 2001), partially covering the topography of a crater floor along with boulders of varying sizes or unconsolidated material (Sears et al., 2015) leaving behind a sharp edge of deposition at the walls of a crater depression (Robinson et al., 2001; Veverka et al., 2001). Further, they form a nearly flat or low slope terrain (usually ~≤10° on Eros) (Cheng et al., 2002) and often have apparent variations with sharp boundaries in albedo relative to the surrounding plains (Robinson et al., 2001). The smooth material is distributed either at the crater floor center and/or is often slightly offset from the geometric center (Robinson et al., 2001) (Figures 1a–1c). The variation in albedo can be due to mineral heterogeneity (Robinson

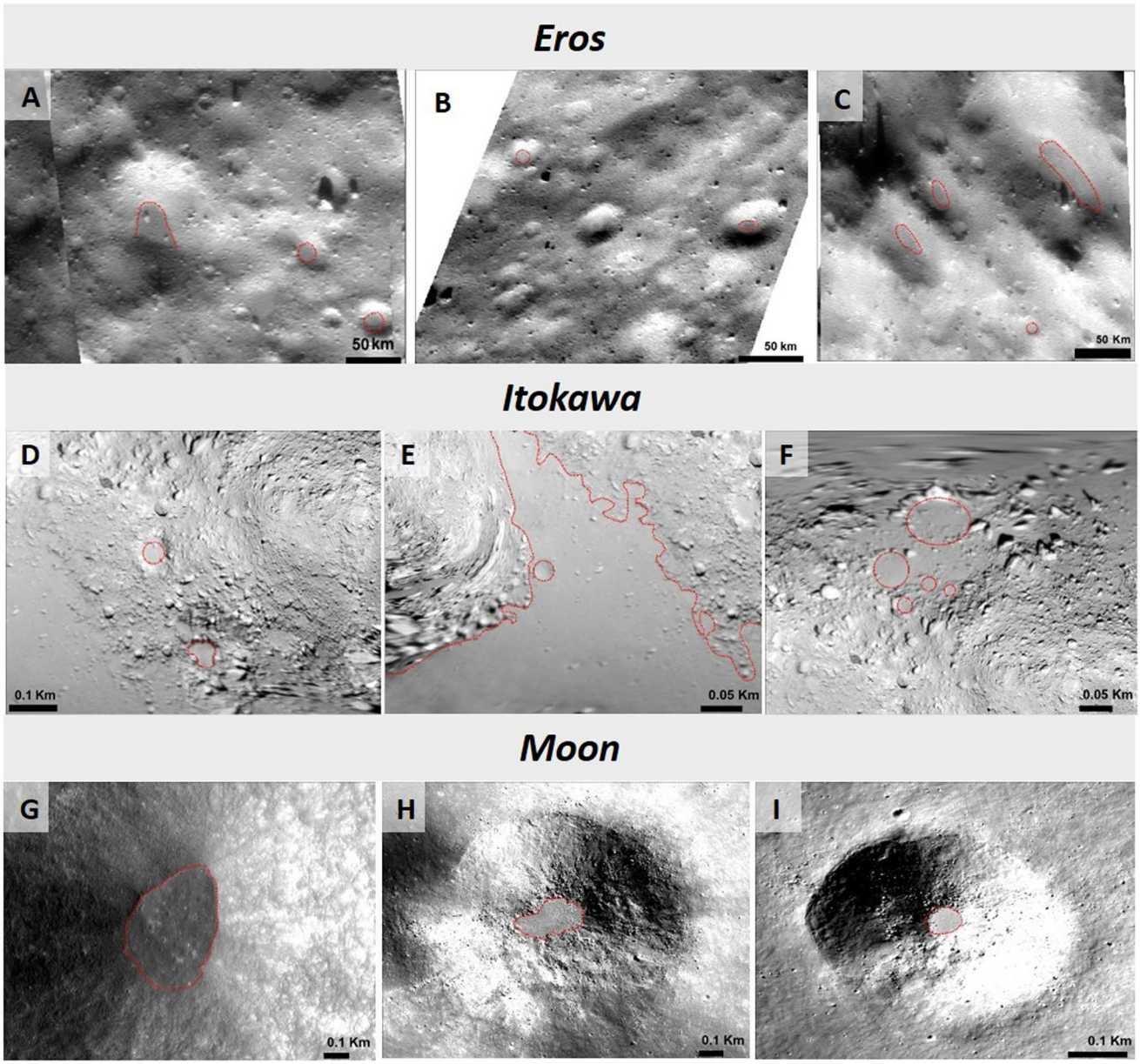

Figure 1. Examples of pond impressions on Eros (a–c), Itokawa (d–f) and the Moon (g–i). The ponded regions are highlighted by red dotted lines. The location of the shown ponds are as follows: (a) long: 175.7°E, lat: 1.61°S; (b) long: 6.56°E, lat: 5.48°S; (c) long: 165.28°E, lat: 3.64°S on Eros; (a) evenly distributed fine material at the crater floor, (b) and (c) identify ponded material at the steepening surface of the crater wall; (d) Komaba crater (long: 102°E, lat: 10°S) and an unnamed flat region; (e) crater like depression present within the large smooth region of Muses Sea and (f) five small circular smooth features located within Uchinoura (long: 40°E, lat: 90°S) on Itokawa. Melt pool exhibiting a smooth surface at the bottom of the crater located at (g) long: 97.5°E, lat: 2.36°N, (h) long: 81.70°E, lat: 32.02°S, (i) long: 235.71°E, lat: 40.6°S on the Moon. The presence of boulders is evident near the ponds' rims in (h) and (i).

et al., 2001), space weathering (Heldmann et al., 2010; Robinson et al., 2001; Sears et al., 2015), or the difference in grain size between the pond regolith and the surrounding region (Heldmann et al., 2010; Robinson et al., 2001). Some of these characteristics of the pond deposits are found not only on Eros but are also identified within large regions (Sagamihara, Muses-Sea) of Itokawa (Fujiwara et al., 2006; Miyamoto et al., 2007; Saito et al., 2006; Yano et al., 2006) (Figures 1d–1f) and small craters on the Moon (Figures 1g–1i) (Hawke & Head, 1977b, 1979; Plescia & Cintala, 2012; Stopar et al., 2012). Overall, ponded regions are noted on planetary bodies with dry brittle regolith and/or low volatile content (Miyamoto et al., 2007; Robinson et al., 2001). However, based on the weathering process, impacts, and regolith material properties of the

Table 1
Physical Characteristics of the Planetary Objects Discussed in This Study (Murdoch et al., 2015)

Planetary body	Size (km)	Bulk density (kg/m^3)	Surface acceleration (m/s^2)
Eros	34.4 × 11.2 × 11.2	2,700	0.0023–0.0056
Itokawa	0.535 × 0.294 × 0.209	1,900	0.000024–0.000086
Moon(dia.)	3,474.8	3,344	1.62
Vesta	572.6 × 557.2 × 446.4	3,500	0.25

different planetary bodies, these geomorphologic appearances may vary and are not necessarily identical in all the identified ponded regions.

Depending on the material properties and identified pond impressions, various geological processes have been suggested as mechanisms to produce ponds on Eros, Itokawa, and the Moon. On Eros, electrostatic levitation and seismic shaking were proposed earlier as a possible formation mechanism for the dust ponds (Cheng et al., 2002; Robinson et al., 2001; Veverka et al., 2001). Electrostatic levitation was proved to be responsible for the mobility of charged particles (Lee, 1996; Roberts et al., 2014; Robinson et al., 2001; Veverka et al., 2001) where as seismic waves induced the segregation to sort grains and produce smooth featureless pond deposits (Cheng et al., 2002; Robinson et al., 2001; Thomas et al., 2002; Veverka et al., 2001). However, both theories fail to explain the distinct distribution of ponds and significant color variation identified within ponded material (Dombard et al., 2010). Later on, Dombard et al. (2010) proposed the boulder disintegration due to space weathering based on the close proximity of large size boulders (upto ∼30 m) with pond deposits. Recent laboratory simulations also suggest the involvement of volatile outgassing as a possible production mechanism for the formation of ponded features on Eros via (a) exogenic volatile-rich meteor impacts or (b) endogenic substances present within subsurface regolith (Sears et al., 2015). Moreover, Eros is a class S asteroid resembling ordinary chondrites (Bell et al., 2002) with the presence of hydrated minerals within chondrites (Grossman et al., 2000; Hutchison et al., 1987). Even though none of the images show direct involvement or geological features of volatile outgassing activity (such as pitted terrains or cracks) on Eros, a possible involvement cannot be excluded.

Similarly, on Itokawa, the Muse-Sea and Sagamihara regions are composed of unconsolidated granular material that was rearranged post-accumulation (Miyamoto, 2014). As on Eros, it is assumed that the surface of Itokawa experiences a similar process of particle segregation (Saito et al., 2006). Given the small size of Itokawa (Table 1), seismic energy generated through impacts can cause global surface vibrations within the regolith (Miyamoto, 2014) which may result in the rearrangement of unconsolidated material. The smooth ponded regions of Itokawa present within the low gravitational potential (Fujiwara et al., 2006) point toward the gravitational movement of fine particles. Similar to Eros, volatile activity is also suspected as one of the potential mechanisms for the pond formation on Itokawa. The assumption was based on the (a) isotope studies of the Hayabusa returned samples which proved that dehydration occurred during the early history of Itokawa within the region of Muse-Sea (Jin & Bose, 2019), (b) prediction models developed by considering the thermal diffusivity and collision history of Itokawa and the anticipated loss of water within Itokawa regolith at depths of 10 m-1 km during its early history (Jin & Bose, 2019) and (c) the presence of circular depression-like geologic features (Saito et al., 2006) (Figures 1d–1f, highlighted in red) which resemble laboratory-generated depressions formed due to volatile fluidization (Sears et al., 2015).

Unlike Eros and Itokawa, the ponded features identified within craters of the Moon are known as "melt pools" and the majority of them are formed from the melting of impact materials (Hawke & Head, 1977a, 1977b, 1979). Cintala and Grieve (1998) derived a model which predicted that high-velocity impactors (∼40 km/s) are capable of producing large volumes of melt that form thin layers in their neighboring regions (Hawke & Head, 1977a, 1977b; Howard & Wilshire, 1975). The ejected melt will then flow to lower elevated regions, forming lobate-like bulge features (Howard & Wilshire, 1975). In such cases, pre-existing topography conditions such as lower height downslope rim crest and evidence of flow margins is required. Nevertheless, only a small percentage of craters (∼6%) reveal lobate flow margins and very few craters have low elevated rim crests allowing such drainage (23 out of 69) (Stopar et al., 2014). Thus, the emplacement of melt material requires certain pre-existing surface conditions for the transport of the impact melts which are not always observed. Other than high velocity, near vertical impact velocity models (Cintala & Grieve, 1998; Pierazzo & Melosh, 2000; Plescia & Cintala, 2012) suggests an alternative explanation that does not require any topographic conditions. According to these models, near vertical impactors produce melt that does not spread outside the crater floor but allows the melt to remain within the crater which later creates smooth flat pond surfaces as the temperature decreases (Plescia & Cintala, 2012). The majority of studies focus on melt formation as a possible mechanism to produce ponds on the lunar surface

(Hawke & Head, 1977a, 1977b; Plescia & Cintala, 2012; Stopar et al., 2014), however, given the dusty regolith of the Moon, the formation of ponds via particle levitation cannot be overlooked. Nevertheless, particle levitation requires a higher degree of electric charging to lift and mobilize dust particles on the Moon (Stopar et al., 2014) compared to smaller bodies like Eros due to the larger gravitational pull (Table 1; Thomas et al., 2002). Furthermore, recent data from the Lunar Atmosphere Dust and Environment Explorer (LADEE) do not show any evidence of a dense dust cloud near the lunar surface (Horányi et al., 2015; Szalay & Horányi, 2015). Thus, impact melt production appears to be the most feasible mechanism to explain the formation of ponded features on the surface of the Moon at a global scale.

In a nutshell, multiple mechanisms including electrostatic levitation (Lee, 1996; Robinson et al., 2001), seismic shaking (Robinson et al., 2001), boulder comminution (Dombard et al., 2010), fluidized impact ejecta (Hawke & Head, 1977b) and volatile outgassing (Sears et al., 2015) are possibly responsible for the formation of pond deposits on Eros, Itokawa, and the Moon.

The asteroid Vesta is a dry planetary object (Jaumann et al., 2012) that was rigorously explored by the Dawn mission. Through this mission, a large number of high-resolution data were collected which enabled us to study and understand the surface of Vesta closely. Vesta's surface consists of a low volatile content regolith with a few morphological exceptions such as pitted terrain (Denevi et al., 2012), gully-like features (Scully et al., 2015) and fluidized impact ejecta (Williams, Denevi, et al., 2014; Williams, O'Brien, et al., 2014) of large craters such as Marcia (~58 km in diameter). Vesta's regolith provides an ideal condition for the formation of ponds, which on Eros and Itokawa required a dry environment. In this study, our objective is to identify and characterize the ponded features on the surface of Vesta, including the material properties and surface conditions under which the ponds form. Further, we compare them with numerous possible material migration and regolith sorting mechanisms identified on Eros, Itokawa, and the Moon to understand their formation and explore the detailed morphology of ponded features.

2. Methods

2.1. Data

For comparison, we adopted the data from previous studies. For Eros, we have used the images collected by the NEAR-Shoemaker spacecraft (Multi-Spectral Imager and Near-Earth Asteroid Rendezvous lander) which has a spatial resolution of ~0.3–0.7 m/pixel. For pond detection, we used geospatial point shapefile data from Robinson et al. (2002). In the case of Itokawa, we used the 0.3 m/pixel imaging mosaic derived from the Gaskell shape model prepared from the Asteroid Multiband Imaging Camera (AMICA) on the Hayabusa mission (Saito et al., 2006). Lastly, for the Moon, the mapped melt pool details are available from Plescia and Cintala (2012). Based on the shared latitude and longitude information, we gathered Lunar Reconnaissance Orbiter Camera (LROC) imaging data of the Moon. The image data has a spatial resolution ranging from 0.1 to 0.9 m/pixel.

For Vesta, we used mosaics from the Low Altitude Mapping Orbit (LAMO) from the Dawn mission's framing camera (Sierks et al., 2011) which has a spatial resolution of ~20 m/pixel (Roatsch et al., 2013). For the topographic information, we overlaid a High-Altitude Mapping Orbit (HAMO) digital terrain model (DTM) with 92 m/pixel lateral spatial resolution (Preusker et al., 2012). The DTM's spatial resolution is coarser than the image resolution, however, given that our smallest craters are 1.4 km in diameter, this is the best available DTM suitable for our analysis. The HAMO DTM is referenced to a best-fit ellipsoid of 286.3 × 278.6 × 223.2 km (Preusker et al., 2012). On the Moon, melt-like ponds are visible in 25 m/pixel images (Plescia & Cintala, 2012) whereas on Eros smooth ponded features can be identified at 0.5 m/pixel (Robinson et al., 2001), and on Itokawa, they are visible at the 50 m scale in images which have resolutions from 0.3-0.7 m/pixel (Hirata et al., 2009). With similar dry regolith present on Vesta, the high resolution of surface data has successfully enabled us to identify pond deposits.

2.2. Criteria for Identification of Pond and Method to Measure Pond Depth

Distinguishing between different types of pond-like landforms can be an arduous task due to their morphologic similarities, especially while using remotely sensed data where confirmation via ground truth is

Table 2
Summary of Ponded Impressions Identified on Vesta, Eros, Itokawa, and the Moon

Ponded characteristics on Vesta	Eros	Itokawa	Moon
Type 1 pond deposit			
Fluidized impact ejecta material	✗	✗	✓
Smooth, nearly flat crater floors	✓	✓	✓
Shallow pond depth	✓	✓	✓
Distributed equipotentially within crater floors	✓	✓	✓
Relatively shallow slope	✓	-	✓
Type 2 pond deposit			
Dry fine-grained material	✓	✓	✗
Uneven ponded surface	✗	✓	✗
Material distributed either within crater floors and/or partially extending to the wall	✓	✗	✗
Increase in slope	✓	✓	✓
Pit like impressions	✗	✗	✗
Relatively deep ponds	✗	✗	✗

impossible. In such instances, researchers need to rely on the geological context present within the datasets. In our study, we considered neighboring geological conditions and previous studies of ponded features on Eros, Itokawa, and the Moon (Roberts et al., 2014; Robinson et al., 2001; Stopar et al., 2014) to understand the contrast in various morphological characteristics of ponded deposits. In general, dust pond deposits on Eros, Itokawa and melt-pools on the Moon have the following common characteristics, but they are not necessarily present in all the ponded candidates: often both types of deposits (a) have superimposed boulders and loose materials, (b) are in general identified in small carters (<1 km in diameter), (c) have a sharp boundary between the ponded deposit and the crater wall, and (d) are equipotential distributed within the crater floor resulting in a smooth surface (Fujiwara et al., 2006; Roberts et al., 2014; Robinson et al.,2001). However, a key difference between both type of ponds is that the dust deposits on Eros and Itokawa comprise fine dry regolith (with grain sizes of mm to cm on Itokawa and <2 cm on Eros), preferentially present near the equator (observed on Eros) and the majority of them are identified in low gravity regions (Cheng et al., 2002; Fujiwara et al., 2006; Robinson et al., 2001; Saito et al., 2006; Thomas & Robinson, 2005; Veverka et al., 2001). In contrast, the ejecta ponds are not correlated with latitude, longitude, or gravitational regions (Plescia & Cintala, 2012; Stopar et al., 2014) and are formed from the fluidized impact ejecta and/or impact melt of a neighboring crater. In Table 1, we list the observed morphological characteristics of ponded features on Eros, Itokawa, and the Moon. While conducting the survey of ponded candidates on Vesta, we consider the characteristics mentioned in Table 2 as a key for identification and further classify them into two categories namely: type 1 and type 2 pond deposits.

Next, we estimate the approximate depth of the ponded material. For this, we use the DTM and derive the current shape of the crater. We then add a least squares fit of a power function (polynomial fit) to the crater walls and estimate the original crater depth (d). Previously, the polynomial fit method has been used to best estimate the depth of sedimentary infilling within simple bowl-shaped craters on Mars (Savage et al., 2018). The difference between the measured shape from the DTM and the fitted original depth is the ponded material depth.

3. Observations and Interpretations

The following sections focus on distinct characteristics of type 1 and type 2 pond deposits on Vesta with concentration to their distribution and morphological evidence. The identified host craters are located within central latitudes (0°–30°N and 0°–25°S) of Vesta. In total, we have identified 10 craters on Vesta which show one or more pond characteristics mentioned in Table 2. These craters have a relatively small diameter (≤11 km) and half of them (5 out of 10) of them are scattered in the southern region of the Marcia (average ~75.3 ± 32 km distance from rim) and northern part of Cornelia crater (2 out of 10 at the average distance

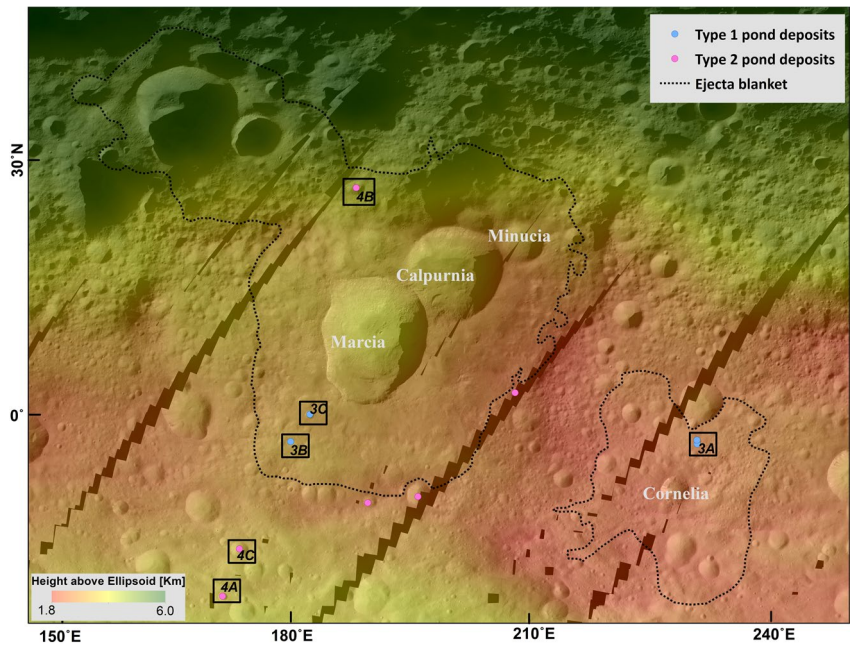

Figure 2. Map of ponded crater identified on the surface of Vesta. Black dotted line represents the ejecta blanket of the nearby large craters, derived from the geological map of Vesta by Williams, Denevi, et al. (2014). All type 1 and type 2 pond deposits are obsereved in and around ejecta blankets. The black boxes indicate the location of areas displayed in Figures 3 and 4 The ponded craters are mapped on a LAMO global mosaic and on a HAMO mosaic (only where high resolution data is not available) on which a HAMO DTM is superimposed (equidistant projection) to understand the surface elevation.

of ~21.6 ± 1 km form the rim) (Figure 2). The derived original depth (d) to diameter (D) ratio of the crater (d/D) is ~0.60 (by assuming simple bowl-shaped fresh craters). This estimation represents the upper limit of the d/D ratio of host craters in which ponded features are observed because most of the craters have experienced some degree of degradation but not all the craters show ponded characteristics. Schenk et al. (2021) measured the current d/D ratio of simple bowl-shaped craters on the Vesta which is ~0.22. The difference in the d/D ratio of original and current craters can be due to resurfacing events that have been taking place in the past. Note that this is an approximate estimation to understand the variation in pond depth within identified crater candidates.

We characterized ponded crater candidates into two categories depending upon their morphology and their position within the craters. Among the identified ponded craters, a few deposits show a shallow slope throughout (≤15°), have a smooth surface with pond material evenly distributed covering the crater floor, the host craters of these pond deposits are located on relatively low elevated regions (blue dots in Figure 2) and in general present within the vicinity of impact ejecta spread (type 1). Such ponds are shallow in depth (average 0.12 km). So far, we identified four craters that exhibit the above-mentioned morphology (Figures 3a–3c). Based on the topographic profiles, we understand that the material infills the lowest region on the crater interior and gradually builds up toward the crater wall, producing a smooth surface. Similar smooth surfaces also appear outside in the vicinity of these carters (Figures 3a–3c). We notice smooth surfaces in the vicinity (v-shaped cuspate toes and furrows highlighted in Figures 3a and 3b), partially broken low-raised rims, and a downslope topography (~2.5 km relief difference) within the host craters' region (Figure 2). Based on this evidence we assume that the material creating the ponds and the neighboring smooth terrain must have originated from the same source. The identified craters in this category are present within the ejecta blanket of nearby larger impact craters (Figure 2). There are a few more small craters observed within ejecta blankets with similar morphology, however, they are not easy to delineate due to lack of strong morphological impressions, unlike the above-mentioned examples. Due to the close proximity of ejecta ponds within Marcia, Calpurnia, Minucia, and Cornelia crater, the combination of impact ejecta and impact melt deposits (Williams, Denevi, et al., 2014) may be the putative source for the ponded deposit

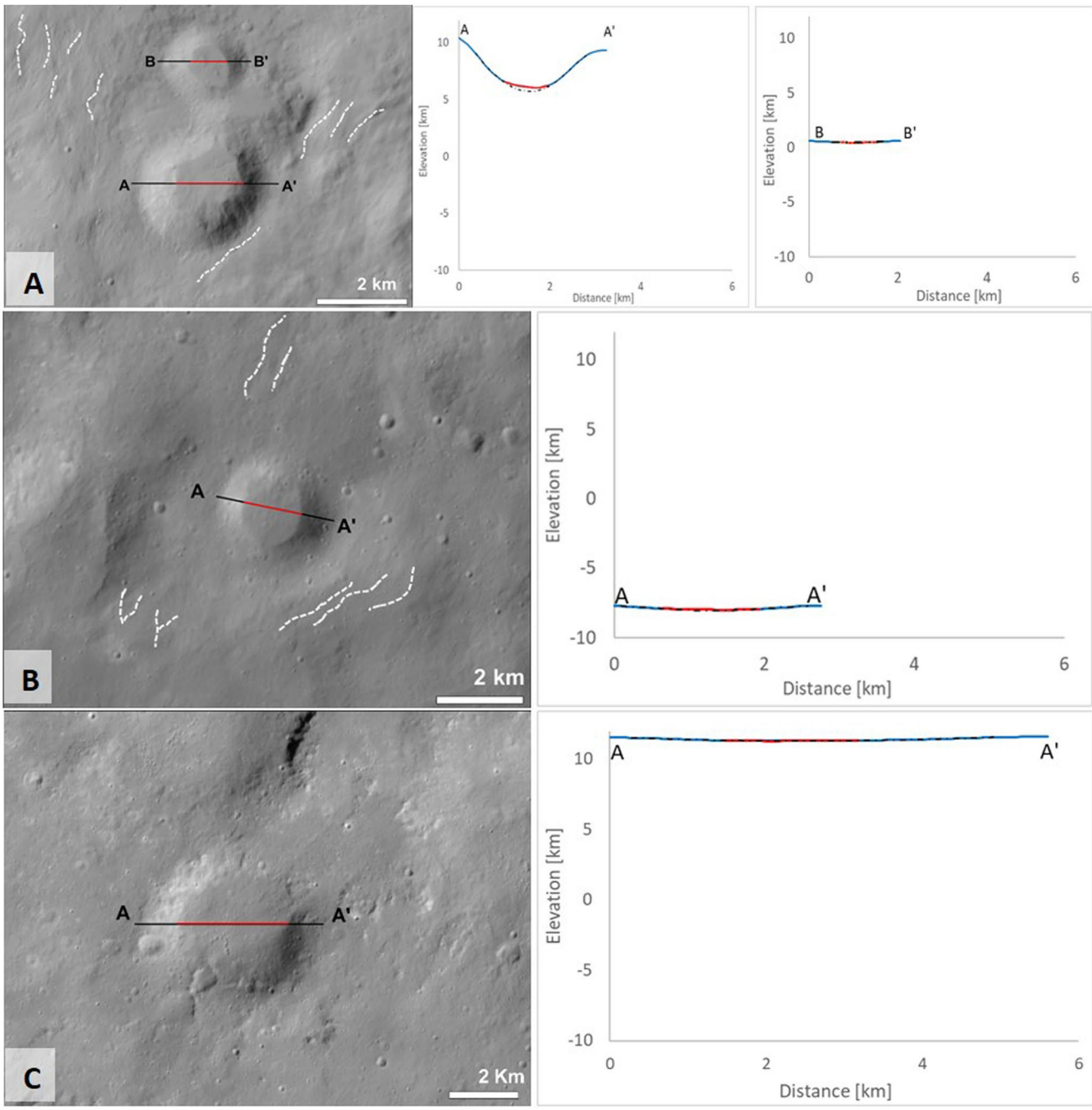

Figure 3. Example of type 1 pond deposit on Vesta. (a) two unnamed craters located south of Cornelia crater with their corresponding surface profile (A-A' and B-B'). The ponded deposit is sharply constrained by the pre-existing crater walls. (b) and (c) are two unnamed ejecta pond hosting craters and their corresponding elevation profile. The craters are located south west of Marcia crater at a distance of ~38.3 and ~20 km from Marcia's crater wall. In the profiles, the blue line denotes the crater shape, red corresponds to the ponded deposit and the black white-doted line indicates the original shape of the crater. In the images (a) and (b) white dashed lines highlight furrows and v-shaped cuspate flow-like impact melt. North is up in all the images.

producing smooth and flat pond surfaces. These pond deposits show all the morphological characteristics similar to 'melt-pools' present on the Moon (Table 2).

Additionally, we found a few ponded features with some different morphological impressions. The ponded deposits within these craters are distributed more heterogeneously, forming an irregular surface with an undulating slope (type 2). In this type, the loose ponded material is located at the base of the crater wall

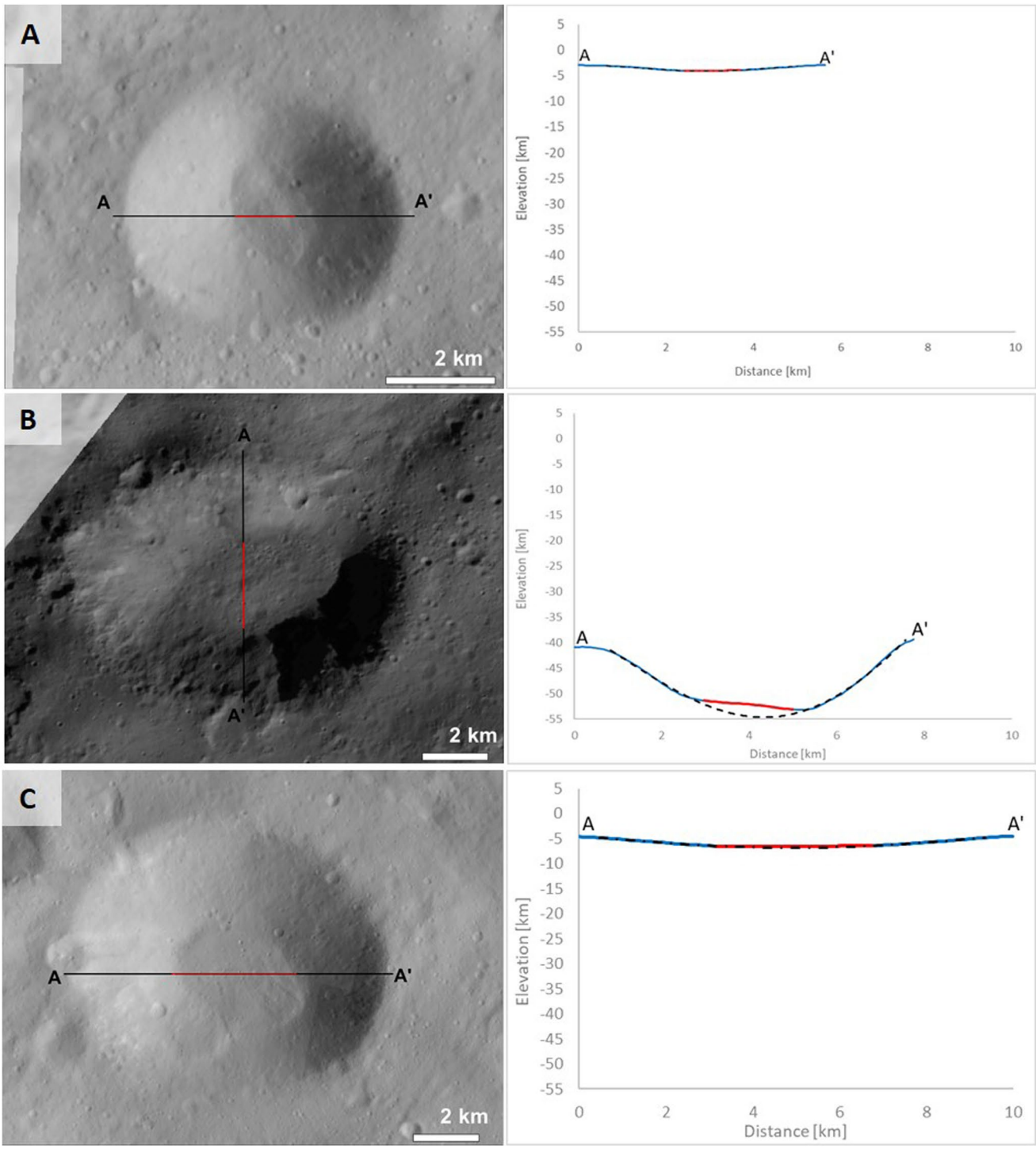

Figure 4. Example of type 2 ponds on Vesta**.** Crater (a, b, c) and their corresponding elevation profile (right) in which the pond is partially extended at the steep wall of the crater. (b) Based on the topographic information, it is evident that the slope in the central region is not flat indicating that the deposit is not (yet) equipotential distributed. (c) Surface of ponded material identified within an unnamed crater and its topographic information shows a gradual increase in elevation. In all elevation examples, the current crater profile is shown in blue, the pond deposit is highlighted in red and the estimated original crater profile is shown as a black dashed-dotted line. North is up in all the images.

Table 3
Characteristics of Ponded Material on Vesta

Pond Id	Lat.	Long.	Floor appearance	Crater floor to wall transition	Slope of ponded material	Pond depth (km)	Distinct change in slope from floor to wall	Surface profile direction	Notes
Type 1: Smooth, featureless deposits evenly distributed at the crater floor, shallow slope within deposit material, host craters located at low elevated regions with low relief topography, shallow pond depth, formed from fluidized impact melt.									
(1)	3.77°S	228.34°E	Flat and smooth	Gradual	≤15°	0.21	no	W-E	Smooth in-flow layer distributed equipotentially at the surface, deep bowl-shaped, following crater topography (Figure 3a, bottom)
(2)	3.20°S	228.34°E	Flat and smooth	Gradual	≤15°	--	no	W-E	Partially covering crater floor in simple bowl shape crater with smooth texture (Figure 3a, top)
(3)	3.24°S	179.40°E	Flat and smooth	Sharp	≤15°	0.05	no	NW-SE	Melt material drained from north east and distributed within lower elevated regions of crater, the prominent striation flow patterns are visible in surrounding regions (Figure 3b)
(4)	0.20°S	181.80°E	Flat and smooth	Sharp	≤15°	0.10	no	W-E	Located nearby Marcia impact crater, the low-raised crater rim from north east provide channel to molten material which covers the entire crater floor (Figure 3c)
Type 2: uneven deposit surface infilled with fine grained material, variation in slope within deposit terrain, pond material is partially extended off form the crater floor and often extended up to crater walls, depth of ponded material is higher.									
(5)	10.61°S	189.2°E	Flat	Sharp	≤15°	0.31	no	NW-SE	Material at the floor is flat but the slope increases toward the crater wall
(6)	10.04°S	194.91°E	Uneven	Sharp	0°–31°	0.2	yes	N-S	Partially infilling the crater floor, spread in E-S direction
(7)	2.53°N	206.51°E	Uneven	Sharp	0°–31°	0.1	yes	N-S	Uneven distribution of pond material elevated toward the crater wall in SE direction
(8)	26.5°N	187.68°E	Uneven	Sharp	≤15°	0.22	no	N-S	Irregular pond surface partially covering floor with possible pits (Figure 4b)
(9)	16.1°S	173.30°E	Uneven	Sharp	≤15°	0.23	no	W-E	Two ponded deposits are observed; (a) at the bottom of the cater floor, (b) at the lower flank of SE crater wall (Figure 4c)
(10)	21.59°S	171.29°E	Uneven	Sharp	0°–31°	0.23	no	W-E	Oval shaped pond deposit emplaced at crater floor (Figure 4a)

or partially extending toward the walls from the floor with a gradually increasing slope and/or is unevenly distributed on the crater floor (Figures 4a–4c). These ponded features appear to not have experienced sufficient leveling mechanism to make entirely smooth surfaces, however, the features still possess the main characteristics of ponds mentioned in prior studies (Robinson et al., 2001) (such as pools of fine-grained regolith, partially extending toward crater walls with a sharp boundary with reference to Table 2) (Roberts et al., 2014; Robinson et al., 2001). In general, these ponds are identified inside relatively large craters (5.90–10.05 km) with estimated average pond depths of ∼0.21 km. For this group of ponds, the feasible source of ponded material is the migration of loose surface material via seismic shaking and/or emplacement of fine regolith from the subsurface via volatile outgassing. Our identified type 2 ponds on Vesta show some resemblance to ponded craters on Eros and Itokawa (Table 2). Both type 1 and type 2 pond deposits have some different and some overlapping impressions which are summarized in Table 3.

4. Comparison of Vesta Ponds With Those on Eros, Itokawa, and the Moon

On Vesta, type 1 and type 2 ponds show various degrees of resemblance with ponded deposits on Eros, Itokawa, and the Moon (Table 2). However, ponded features on Eros and Itokawa are produced from fine dust substances whereas similar features are formed from molten and fluidized impact melt material on the surface of the Moon.

On Eros, 334 ponded deposits were identified, but due to limitations in data resolution, only a minority of them (in this Case 55) were analyzed in detail (Robinson et al., 2002). In terms of morphology, there are a few similarities between ponded features of Eros and Vesta, but differences are observed within their geometrical assessments. On Vesta, the majority of ponded craters are identified within similar latitudes as on Eros (0°–30°S/N). According to Roberts et al. (2014) out of 55, only 12 ponds have a flat smooth surface (≤10° slope) with an equipotential distribution of fine material at the crater floor (Figure 1a) and a shallow depth similar to ejecta ponds on Vesta. On Eros, there are no ejecta ponds. However, in visual interpretation, the smooth surface of dust ponds on Eros appears similar to the smooth surface of ejecta ponds on Vesta. The remaining 43 ponds are identified on steep crater walls or are partially elongated (Figures 1b and 1c), resembling dust ponds on Vesta. Nevertheless, the main difference is the size of the ponds and the potential source of ponded material. In general, the lower limit of the pond diameter is >30 m and is present within craters of <1 km diameter on Eros (Robinson et al., 2001). Further, the ponded deposits infill only a few meters of the original depth of the crater (Robinson et al., 2001) on Eros. Whereas on Vesta, the diameters of ponds range from 0.9 to 6.4 km within larger craters (~2–10 km). The overall pond depth is ~0.2 km on Vesta and covers a maximum of up to ~10% of the crater depth. The smaller size of ponded craters on Eros might be due to the significant size difference and consequently gravitational force between Eros and Vesta. Moreover, the majority of the ponds are present within low gravitational regions on Eros (Robinson et al., 2001, 2002), however, Vesta's gravitational field is comparatively even.

On Itokawa, the surface also shows smooth flat pond regions and depressions. These smooth regions were described as featureless and consisted of a fine regolith layer (Fujiwara et al., 2006; Miyamoto et al., 2007; Saito et al., 2006; Yano et al., 2006). So far 28 craters (out of 38; Hirata et al., 2009) show a morphology that has similar characteristics to dust and ejecta ponds of Vesta. The typical ponded feature on Itokawa includes smooth featureless fully or partially covered crater floors with low raised, brighter rims (Saito et al., 2006) and fine infilling material (~6 cm particle size) (Figures 1d–1f). On Vesta similar characteristics are present within both the category of ponded deposits (such as flat smooth surface within type 1 and fine-grained infilling material within type 2). The identified pond features on Itokawa are more abundant in small craters (0.002–0.134 km in diameter) (Hirata et al., 2009). A strong correlation between color and albedo variation was observed and is possibly sensitive toward the grain sizes within regolith material (Saito et al., 2006). Other than the craters, the Sagamihara and Muses Sea regions also show smooth featureless ponded deposits (Fujiwara et al., 2006) (Figure 1e) and occupy ~20% of the total asteroid surface (Hirata et al., 2009; Yano et al., 2006). Nevertheless, unlike Vesta, Itokawa reveals no obvious evidence of type 1 ponds. The overall generation of smooth pond-like impressions involves migration of dry regolith (Fujiwara et al., 2006; Miyamoto et al., 2007; Saito et al., 2006) on Itokawa.

Characteristics of ponded materials were also identified within craters on the Moon (Hawke & Head, 1977a, 1977b; Howard & Wilshire, 1975; Plescia & Cintala, 2012). Previous studies by Howard and Wilshire (1975) reported on the presence of flat featureless ponded material within small craters (diameters of 1–5 km). Fluidized ejecta melt for the production of ejecta ponds was proposed by Hawke and Head (1977a, 1977b). They noted that craters with less than a certain diameter (<5 km) do not possess ponded deposits. However, this study was conducted in relatively low-resolution data. Later on, Plescia and Cintala (2012), used the LROC data set to conduct a global survey of small craters (up to 0.12 km in diameters) and cataloged features as "melt pools." Stopar et al. (2014) observed similar smooth deposits outside crater rims and concluded that they must be produced from the fluidized ejecta melt. The molten material exhibits flat-floors with a smooth texture, a sharp increase in slope from floor to wall, a heterogeneous distribution of boulders at the rim of the pond, and infilling of the deepest region of the crater floors with molten substances (Figures 1g–1i). We identified similar features as type 1 ponds on Vesta. Depending upon the thickness of pool deposits, boulders, and hummocky material can also be seen partially buried within the melted region on the Moon (Figures 1h and 1i). The identified host craters with ponds on the Moon have

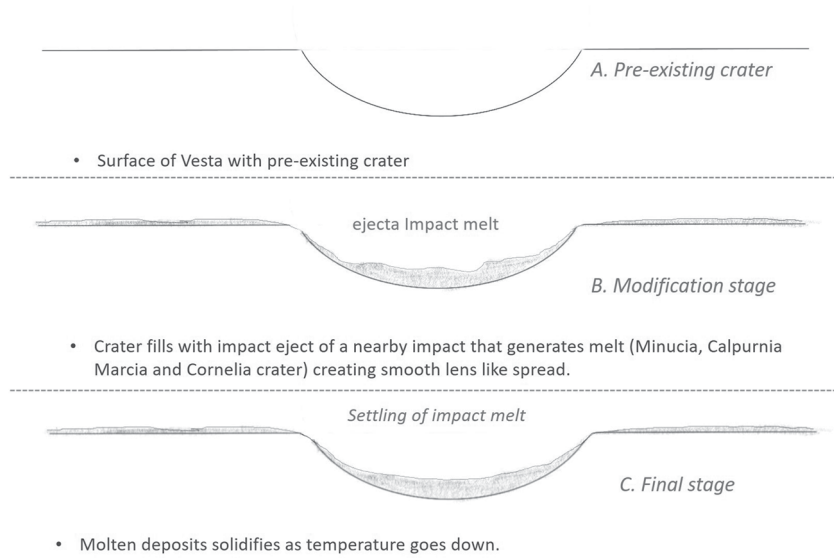

Figure 5. Illustration of production of type:1 ponds via emplacement of impact melt. The ejecta ponds on Vesta can be formed via downslope movement of ejecta melt material from neighboring impact crater ejecta. The ejecta infills the lower cavity of the crater and later solidifies.

diameters from 0.12 to 30 km and pool diameters of 0.007–6 km (Plescia & Cintala, 2012). In comparison to Vesta, the impact melt on the Moon is much more prevalent due to higher impactor energies caused by higher velocities of the impactors (40 km/s), derived via theoretical models (French, 1998). So far, the literature predominantly suggests the presence of melt pools on the Moon.

5. Hypothesized Processes for the Production of Type 1 and Type 2 Ponds on Vesta

Both the pond deposits on Vesta reveal partially overlapping features with the ponded morphology noted on Eros, Itokawa, and the Moon. However, their formation mechanism and material properties are different. Based on our observation and comparison with ponded characteristics on other planetary objects, we understand that both types of ponds on Vesta must have undergone different formation mechanisms.

Type 1 pond deposits show a flat smooth homogenous distribution of the flow-like impact melt material (Figures 3a and 3b) within the crater floor which is commonly identified on the surface of the Moon. The melt materials are well preserved in and around the vicinity of the impact craters. The craters hosting the ejecta ponds on Vesta are underneath the sheet of the ejecta blanket. They are typically shallow and located within relatively small craters producing a smooth lens-like surface at the bottom of the crater cavity. Similar to ejecta ponds on the Moon, craters hosting type 1 ponds on Vesta too have low raised rims (average ~0.04 km in height) and are located on the lower elevated region which provides ideal topographic conditions for the downslope movements of melts. According to the stratigraphy and age models of the Marcia crater region, the northernmost Minucia crater must be the oldest crater followed by the Calpurnia crater and Marcia (Williams, Denevi, et al., 2014). Geological and spectral evidence gathered from the Dawn data also suggests that the ejecta melt in this region is composed of the impact ejecta of Minucia, Calpurnia, and Marcia (McCord et al., 2012; Williams, Denevi, et al., 2014). Thus, based on the apparent age and the morphological evidence of melt material, we hypothesize that given the close proximity of the ponds to the region that has been identified as melt-rich, the ponds are melted from Marcia, Calpurnia, and Minucia that gathered in pre-existing craters. A similar impact melt infilling process may apply to the ponds identified on the north of Cornelia crater (Figures 2 and 3a). Additionally, the pond-hosting craters are located in lower elevated regions in comparison to Cornelia which makes a possible downslope movement of flow-like impact melt material likely. Due to the similar characteristics of the melt pools of the Moon and type 1

pond deposits on Vesta we name them as "ejecta ponds." We illustrate the formation mechanism of ejecta ponds with a graphical sketch in Figure 5. Other than the impact melt infilling process, we also consider the near vertical high velocity impact theory proposed for melt pool formation on the Moon. However, given the location of Vesta within the asteroid belt and the comparatively low velocities within the asteroid belt, Vesta has experienced relatively slow impacts (~8–10 km/s) (O'Brien & Sykes, 2011; Williams, O'Brien, et al., 2014) in comparison to the lunar surface. Thus, direct melt pool formation in near-vertical high speed impacts as suggested on the Moon is unlikely for Vesta. Additionally, if this mechanism was dominant on Vesta, there should be more ponded craters present on the surface of Vesta at a global scale, but that is not the case.

Type 2 shows resemblance with dust deposits of Eros and Itokawa, however, they are often less flat and smooth. Based on the surface morphology and multi-step seismic model results, it was demonstrated that seismic reverberation on Eros and Itokawa is able to destabilize the slope, cause the regolith to move downslope and form pond deposits (Richardson et al., 2004, 2005; Veverka et al., 2001). Thus, we suspect similar processes may account for type 2 pond formation on Vesta. Due to seismic shaking the fine material may drift from parts of the rim and/or the crater wall and serve as a source for the type 2 pond deposit. Once the deposits are transported downslope, the next step is segregation of fine-grained material. However, unlike type 1 pond deposits, type 2 does not show smooth nearly flat pond deposits at the center of the crater floors. Thus, we suggest that after moving downslope, the dusty material did not undergo a sorting process to form a smooth deposit. To support this hypothesis, we compare the process of Vesta with dusty regolith bearing asteroids. On Eros too, few dust pond candidates (approximately 20%) lack the smooth morphology (Roberts et al., 2014). The absence of a smooth pond morphology is possible either due to an insufficient amplitude of seismic shaking and/or the duration of the shaking that might have lasted only to transport the dusty material downslope (Roberts et al., 2014) but not smoothen it. Thus, to understand diffusivity of the impact-induced seismic shaking, a series of numerical shake-table experiments were conducted (Richardson & Kedar, 2013; Richardson et al., 2020). According to the results, the small size impactors (diameter of 4–500 m for Eros and 0.07–0.5 m for Itokawa) are capable of producing global-scale seismic shaking which then diffuses (at the average peak rate of $\sim 0.5 \pm 0.2$ km^2/s and $\sim 0.002 \pm 0.001$ km^2/s) maximum up to the distance of 20 and 0.62 km on Eros and Itokawa, respectively. Nevertheless, the derived diffusion rate is still of inadequate amplitude to generate a flat-floored pond deposit morphology at a global scale on Eros (Roberts et al., 2014). Given the size of Minucia, Calpurnia, and Marcia craters on Vesta, rare but relatively large-scale impactors (de Elía & Di Sisto, 2011) with similar velocities are expected to generate higher seismic shaking and diffusivity locally. Post-impact seismic energy dispersion may have possibly disturbed the stable conditions and induced the downslope movements of dust. However, to achieve a smooth morphology, separation of grains via segregation would require seismic diffusion for a relatively long time. Since only 6% of the total impactor has a velocity of ~8 km/s (Williams, O'Brien, et al., 2014), frequent repetition of high amplitude seismic dispersion is not expected on Vesta. Moreover, the global scale seismic diffusion is applicable to the asteroids with ≤50 km in diameter, on larger asteroids only local seismic shaking and diffusion are expected (Richardson et al., 2020). Thus, large impacts on the surface of Vesta are not capable of diffusing seismic energy at a global scale. From the above arguments, it is clear that smaller asteroids' surfaces (such as Eros, Itokawa) vibrate more significantly than the larger asteroids (Marchi et al., 2015; Murdoch et al., 2015; Richardson et al., 2004, 2005) for a given impactor size. Additionally, the Small Body Cratered Terrain Evolution Model (SBCTEM) also suggested that at given seismic diffusivity ($\sim 0.5 \pm 0.2$ km^2/s), a 0.04 km diameter crater experiences a gradual infilling process and requires energy diffusion for ~10 Myr to produce smooth pond morphology on Eros (Richardson & Abramov, 2020). On Vesta, our observed host craters have significantly higher diameters (5.90–10.05 km) which will require even more time along with higher attenuation of seismic diffusivity. Considering the massive size of Vesta and large diameter of pond hosting craters, we suspect rare high-amplitude seismic diffusivity at localized scale might be adequate to transport the material downslope but not able to develop smooth, nearly flat pond deposits due to infrequent large impactors. Another potential mechanism for regolith transport on Vesta is the volatile-induced outgassing of the material from the subsurface (Sears et al., 2015). This process is expected only on planetary bodies which had volatile bearing regolith (Benoit et al., 2003). The volatile-induced fluidization process can be triggered either by the impact that produced the host crater excavating volatile-rich material which subsequently degasses and fluidizes the regolith grains (Sears et al., 2015) or by the implantation of thermal energy via impact that may

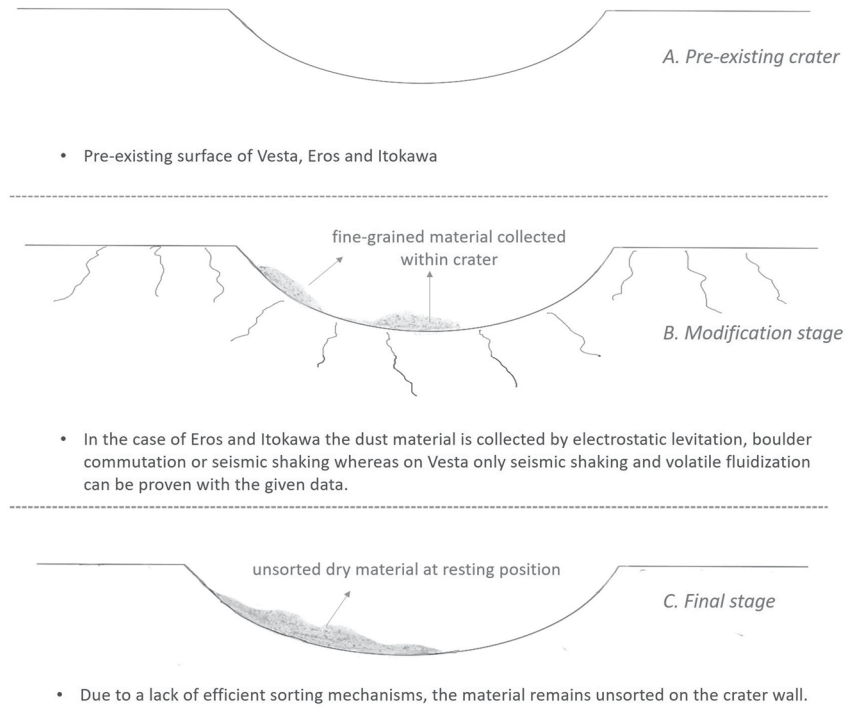

Figure 6. Illustration of production type:2 ponds via seismic shaking. Two possible mechanisms may be responsible for the production of dust ponds, depending upon the environment of the planetary body. Previous studies explain the involvement of all three mechanisms (electrostatic levitation, seismic shaking or boulder commutation) on the surface of Eros (Cheng et al., 2002; Robinson et al., 2001; Thomas & Robinson, 2005; Veverka et al., 2001) and Itokawa (Fujiwara et al., 2006; Saito et al., 2006). But in the case of Vesta a low degree of seismic shaking and volatile-induced outgassing (illustrated by Sears et al., 2015) is probably responsible for the mobility of fine-grained material into the crater.

release mineral-bound hydroxyl groups (and/or other volatiles). Under laboratory conditions, it has been proven that fluidization by gas flow at subsurface scale lifts the individual grains, resettles them on the surface, and produces fine-grained dust ponds on asteroids (Benoit et al., 2003; Sears et al., 2015). Based on the morphological evidence, a small amount of localized volatile presence is strongly suggested on Vesta (Denevi et al., 2012; Scully et al., 2015). However, they cannot survive for a longer time (Scully et al., 2021). Therefore, type 2 pond formation on Vesta may also be possible via one or more of the above-described mechanisms. Both cases are likely to be relatively quick and the pond material might not experience severe sorting or segregation post-accumulation. This may also lead to a not well-established equipotential alignment of dry pond material. The dry brittle regolith condition of Vesta also provides favorable conditions for electrostatic particle levitation (Lee, 1996; Roberts et al., 2014; Robinson et al., 2001; Veverka et al., 2001) and boulder disintegration (Dombard et al., 2010) which are suggested as a potential mechanism for the formation of dust ponds on Eros. Given the higher gravity, larger size (Table 1; Russell et al., 2012), and high escape velocity (~363 m/s; Veverka et al., 2000) of Vesta, the particle levitation and their segregation is not possible. Next, our mapped type 2 ponds do not reveal any large differences in their surface area and lack the presence of boulders within their depressions at a given resolution. Thus, the boulder disintegration mechanism may not be applied in the case of Vesta. The available data has a different spatial resolution for Vesta, Eros, and Itokawa which may have hindered the analysis and made a direct comparison difficult. It is totally possible that there are Eros and Itokawa like ponds on Vesta, but we simply do not see them. Nevertheless, we can still make a comparison to discuss the different processes. The ponded material of this particular group of craters consists of loose fragmented dust-like dry particles and are closely related to pond deposits on Eros and Itokawa, thus we name them as "dust ponds."

Both type 1, ejecta pond and type 2, dust ponds are identified within a similar region on Vesta's surface. However, we comprehend that both of them were produced via different mechanisms. Ejecta ponds show flat-

Table 4
Summary of Possible Geological Processes Responsible for the Production of Ponds on Vesta, Eros, Itokawa, and the Moon

Geological Process	Vesta	Eros	Itokawa	Moon
Dust pond deposit via volatile outgassing	Likely (this work, e.g. nearby pitted terrains)	Possible, hypothesized under laboratory conditions (Sears et al., 2015), but Eros is a dry S-type asteroid and so far, no direct morphological evidences for volatiles are found	Possible, but unbound volatiles are not present, as this process has been suggested to work for Eros, it should work for Itokawa too	Possible, because volatiles are present in the lunar regolith (Basilevsky et al., 2012), but not reported in literature in relation to ponds
Migration of dust via seismic shaking	Since the surface of Vesta has been heavily bombarded, seismic shaking is possible	Eros' regolith has experienced impacts, due to its small size, seismic waves may propagate through the entire body (Robinson et al., 2001;2004)	Due to seismic shaking granular material may have fallen from higher elevated regions into depressions (Fujiwara et al., 2006).	The surface of the Moon has experienced impacts which have the capacity to generate seismic waves (Plescia and Cintala, 2012)
Material segregation via seismic shaking	Unlikely due to the large size of the body, this phenomenon might not be observable due to limitation in the resolution of the data	Possible (Cheng et al., 2002; Robinson et al., 2001; 2004 ; Thomas et al., 2002; Veverka et al., 2001a)	Smooth terrains likely involve processes for grain-size sorting via seismic shaking initiated by impacts (Fujiwara et al., 2006; Saito et al., 2006)	No evidence of dust sorting mechanism noted using current data.
Material segregation via electrostatic forces	Unlikely due to large distances to be travelled and the topography that would need to be overcome electrostatic charging has not been suggested to be a dominant process either	Pond deposits follow underlying topography because of the low gravity and this mechanism is possible for ponds which are not leveled or flatten (Lee, 1996; Roberts et al., 2014; Robinson et al., 2001; Veverka et al., 2001a)	As this mechanism is possible for Eros, it should also be possible for Itokawa. The fine material may have been levitated but high escape velocity (10-20 cm/s) restrict the particle rearrangement (Miyamoto et al., 2007)	Unlikely due to the high gravitational pull and a lack of evidence for a dust cloud near the lunar surface (Horányi et al., 2015; Stopar et al., 2014; Szalay and Horányi, 2015)
Boulder disintegration	Unlikely because there are not enough large boulders to fill an entire crater pond	Thermally disaggregated boulders have been proposed (Dombard et al., 2010)	This mechanism has not been suggested, but given that it is possible on Eros, it should also be possible on Itokawa	Unlikely because there are not enough large boulders to fill an entire crater pond
Ejecta pond infilling via fluidized ejecta (melt and/or volatiles)	Likely, since impact melt has been observed near ponded craters (Williams et al., 2014b)	Unlikely because melt does not occur in impact craters	Unlikely because melt does not occur in impact craters	Likely, impact melt has been observed near ponded craters (Hawke and Head, 1977a; b; Plescia and Cintala, 2012; Stopar et al., 2014)

Note. The colors represent the likelihood with which the geologic processes occur: Green: possible, Orange: may or may not be possible, and red: highly unlikely.

tened surfaces and are evenly distributed within crater floors whereas dust ponds are unlevelled and present on steep regions of the crater hosting the pond. We interpret that ejecta ponds must have formed via infilling of ejecta from the neighboring large craters (Minucia, Calpurnia, Marcia, and Cornelia) which later solidified as part of the crater evolution process (Figure 5). Whereas for the production of the dust ponds, rare high-amplitude localized seismic diffusion and/or volatile-induced fluidization may be responsible for the transportation of granular material downslope (Figure 6). Nevertheless, given Vesta's size, the transported dust material may not have experienced enough seismic shaking allowing the grainy regolith to remain unlevelled and only partially distributed across the crater floor. As a consequence, the typical smooth surface as observed on Eros or Itokawa may not be achieved in dust ponds on Vesta. In Table 4 we have summarized all possible pond formation mechanisms discussed so far on Vesta, Eros, Itokawa, and the Moon.

6. Conclusion

In analogy to investigation on asteroids Eros, Itokawa, and the Moon, we have identified two types of ponded features in craters on Vesta which show some different and some overlapping geomorphologic characteristics. These ponded deposits have experienced different formation mechanisms. Type 1 are ejecta ponds which have a smooth and flat surface with a constant slope and shallow infilling deposits (average ∼0.1 km). They retain the original shape of the crater and the material is evenly distributed within the crater floor. Crater hosting ejecta ponds are possibly formed by the distribution of impact ejecta of nearby craters (Minucia, Calpurnia, Marcia and Cornelia) on Vesta. They are similar to the melt pools identified on the Moon. The pre-existing topography (e.g., low raised rims and location of host crater in low elevated regions) plays a vital role in channelizing and downslope movement of the melt material. Type 2 are dust ponds that have a few different characteristics (in comparison to type 1 ponds) such as granular pond material, pond deposits with undulating surfaces, often relatively greater depth (average ∼0.2 km), and sometimes an abrupt change in slope. The type 2 ponded material on Vesta either moved downwards from parts of crater walls via seismic shaking or may have been transferred onto the surface through volatile outgassing. In the case of seismic activity, the energy diffusion is restricted to a local scale due to the large size of Vesta. Additionally, the surface has not experienced large-scale impactors frequently. Thus, a rare high-amplitude of seismic diffusivity is not capable to conduct particle segregation and produce smooth morphology is relatively huge host craters. Similarly, the presence of volatiles on Vesta is observed at a regional scale (Denevi et al., 2012; Scully et al., 2015) but they might have survived for a shorter time (Scully et al., 2021). Therefore, we interpret that type 2 pond material was transported downslope via seismic diffusivity and/or volatile outgassing. However, the transported material might not experience severe sorting or segregation post-accumulation due to rare high amplitude seismic diffusivity and a short span of volatile activity, thus failing to produce the smooth featureless ponded surfaces as observed on Eros and Itokawa.

Data Availability Statement

Raw images used in this work for Eros (Robinson & Carcich, 2001), Itokawa (Stooke, 2015), and calibrated data from Dawn at Vesta (Nathues et al., 2011) are available at Small Bodies Node of Planetary Data System (PDS). Additionally, we also utilized the pond catalogue of Eros (Roberts, 2021) available at PDS. Derived data products are available via Figshare: Parekh, R. (2021): Formation of ejecta and dust pond deposits on asteroid Vesta (https://doi.org/10.6084/m9.figshare.16863478.v2).

Acknowledgments
The authors acknowledge the Dawn team for providing data and support. This work is part of the research project "The Physics of Volatile Related Morphologies on Asteroids and Comets". RP and KO would like to gratefully acknowledge the financial support and endorsement from the German Academic Exchange Service (under DLR-DAAD PhD Fellowship) and the DLR Management Board Young Research Group Leader Program by the Executive Board Member for Space Research and Technology. A portion of the work was carried out at the Jet Propulsion Laboratory under contract with NASA. Open access funding enabled and organized by Projekt DEAL.

References

Basilevsky, A., Abdrakhimov, A., & Dorofeeva, V. (2012). Water and other volatiles on the Moon: A review. *Solar System Research*, *46*, 89–107. https://doi.org/10.1134/S0038094612010017

Bell, J. F., Izenberg, N. I., Lucey, P. G., Clark, B. E., Peterson, C., Gaffey, M. J., et al. (2002). Near-IR reflectance spectroscopy of 433 Eros from the NIS instrument on the NEAR mission: I. Low phase angle observations. *Icarus*, *155*(1), 119–144. https://doi.org/10.1006/icar.2001.6752

Benoit, P., Hagedorn, N., Kracher, A., Sears, D. W. G., & White, J. (2003). *Grain size and density sepration on asteroids: Composition of seismic shaking*. LPSC XXXIV.

Cheng, A. F., Izenberg, N., Chapman, C. R., & Zuber, M. T. (2002). Ponded deposits on asteroid 433 Eros. *Meteoritics and Planetary Science*, *37*, 1095–1105. https://doi.org/10.1111/j.1945-5100.2002.tb00880.x

Cintala, M. J., & Grieve, R. A. F. (1998). Scaling impact-melt and crater dimensions: Implications for the lunar cratering record. *Meteoritics & Planetary Science*, *33*, 889–912. https://doi.org/10.1111/j.1945-5100.1998.tb01695.x

de Elía, G., & Di Sisto, R. (2011). Impactor flux and cratering on Ceres and Vesta: Implications for early solar system. *Astronomy & Astrophysics*, *534*, A129. https://doi.org/10.1051/0004-6361/201117543

Denevi, B. W., Blewett, D. T., Buczkowski, D. L., Capaccioni, F., Capria, M. T., De Sanctis, M. C., et al. (2012). Pitted terrain on Vesta and implications for the presence of volatiles. *Science*, *338*, 246–249. https://doi.org/10.1126/science.1225374

Dombard, A. J., Barnouin, O. S., Prockter, L. M., & Thomas, P. C. (2010). Boulders and ponds on the Asteroid 433 Eros. *Icarus*, *210*, 713–721. https://doi.org/10.1016/j.icarus.2010.07.006

French, B. M. (1998). *Traces of catastrophe: A handbook of shock-metamorphic effects in terrestrial meteorite impact structures. LPI Contribution No. 954* (p. 120). Lunar and Planetary Institute. Retrieved from https://www.lpi.usra.edu/publications/books/CB-954/CB-954.pdf

Fujiwara, A., Kawaguchi, J., Yeomans, D. K., Abe, M., Mukai, T., Okada, T., et al. (2006). The rubble-pile asteroid Itokawa as observed by Hayabusa. *Science*, *312*, 1330–1334. https://doi.org/10.1126/science.1125841

Grossman, J. N., Alexander, C. M. O. D., Wang, J., & Brearley, A. J. (2000). Bleached chondrules: Evidence for widespread aqueous processes on the parent asteroids of ordinary chondrites. *Meteoritics and Planetary Science*, *35*, 467–486. https://doi.org/10.1111/j.1945-5100.2000.tb01429.x

Hawke, B. R., & Head, J. W. (1977a). Impact melt in lunar crater interiors. In *Presented at the Proceedings of the Lunar and Planetary Science Conference* (p. 415). Retrieved from http://articles.adsabs.harvard.edu/pdf/1977LPI.....8..415H

Hawke, B. R., & Head, J. W. (1977b). *Impact melt on lunar crater rims* (p. 815). Pergamon Press, Inc. Retrieved from http://adsabs.harvard.edu/full/1977iecp.symp..815H

Hawke, B. R., & Head, J. W. (1979). *Impact melt volumes associated with lunar craters* (p. 510). Retrieved from https://ui.adsabs.harvard.edu/abs/1979LPI....10

Heldmann, J. L., Conley, C. A., Brown, A. J., Fletcher, L., Bishop, J. L., & McKay, C. P. (2010). Possible liquid water origin for Atacama Desert mudflow and recent gully deposits on Mars. *Icarus*, *206*(2), 685–690. https://doi.org/10.1016/j.icarus.2009.09.013

Hirata, N., Barnouin-Jha, O. S., Honda, C., Nakamura, R., Miyamoto, H., Sasaki, S., et al. (2009). A survey of possible impact structures on 25143 Itokawa. *Icarus*, *200*, 486–502. https://doi.org/10.1016/j.icarus.2008.10.027

Horányi, M., Szalay, J. R., Kempf, S., Schmidt, J., Grün, E., Srama, R., & Sternovsky, Z. (2015). A permanent, asymmetric dust cloud around the Moon. *Nature*, *522*, 324–326. https://doi.org/10.1038/nature14479

Howard, K. A., & Wilshire, H. G. (1975). Flows of impact melt at lunar craters. *Journal of Research of the U. S. Geological Survey*, *3*, 237. Retrieved from https://pubs.usgs.gov/journal/1975/vol3issue2/report.pdf

Hutchison, R., Alexander, C. M. O., & Barber, D. J. (1987). The Semarkona meteorite: First recorded occurrence of smectite in an ordinary chondrite, and its implications. *Geochimica et Cosmochimica Acta*, *51*(7), 1875–1882. https://doi.org/10.1016/0016-7037(87)90178-5

Jaumann, R., Williams, D. A., Buczkowski, D. L., Yingst, R. A., Preusker, F., Hiesinger, H., et al. (2012). Vesta's shape and morphology. *Science*, *336*, 687–690. https://doi.org/10.1126/science.1219122

Jin, Z., & Bose, M. (2019). New clues to ancient water on Itokawa. *Science Advances*, *5*, 8106. https://doi.org/10.1126/sciadv.aav8106

Lee, P. (1996). Dust levitation on asteroids. *Icarus*, *124*, 181–194. https://doi.org/10.1006/icar.1996.0197

Marchi, S., Chapman, C. R., Barnouin, O. S., Richardson, J. E., & Vincent, J. B. (2015). Cratering on asteroids. In P. Michel, F. E. DeMeo, & W. F. Bottke (Eds.), *Asteroids IV* (pp. 725–744). University of Arizona Press. https://doi.org/10.2458/azu_uapress_9780816532131-ch037

McCord, T. B., Li, J.-Y., Combe, J.-P., McSween, H. Y., Jaumann, R., Reddy, V., et al. (2012). Dark material on Vesta from the infall of carbonaceous volatile-rich material. *Nature*, *491*, 83–86. https://doi.org/10.1038/nature11561

Miyamoto, H. (2014). Unconsolidated boulders on the surface of Itokawa. *Planetary and Space Science*, *95*, 94–102. https://doi.org/10.1016/j.pss.2013.06.016

Miyamoto, H., Yano, H., Scheeres, D. J., Abe, S., Barnouin-Jha, O., Cheng, A. F., et al. (2007). Regolith migration and sorting on asteroid Itokawa. *Science*, *316*, 1011–1014. https://doi.org/10.1126/science.1134390

Murdoch, N., Sanchez, P., Schwartz, S., & Miyamoto, H. (2015). Asteroid surface geophysics. In *Asteroids IV* (pp. 767–792). https://doi.org/10.2458/azu_uapress_9780816532131-ch039

Nathues, A., Sierks, H., Gutierrez-Marques, P., Schroeder, S., Maue, T., Buettner, I., et al. (2011). *DAWN FC2 CALIBRATED VESTA IMAGES V1.0, DAWN-A-FC2-3-RDR-VESTA-IMAGES-V1.0, NASA planetary data System*. Retrieved from https://sbn.psi.edu/pds/resource/dawn/dwnvfcL1.html

O'Brien, D. P., & Sykes, M. V. (2011). The origin and evolution of the asteroid belt—Implications for Vesta and Ceres. *Space Science Reviews*, *163*, 41–61. https://doi.org/10.1007/s11214-011-9808-6

Pierazzo, E., & Melosh, H. J. (2000). Melt production in oblique impacts. *Icarus*, *145*, 252–261. https://doi.org/10.1006/icar.1999.6332

Plescia, J. B., & Cintala, M. J., (2012). Impact melt in small lunar highland craters, *Journal of Geophysical Research*, *117*. https://doi.org/10.1029/2011JE003941

Preusker, F., Scholten, F., Matz, K.-D., Roatsch, T., Jaumann, R., Raymond, C. A., & Russell, C. T. (2012). *Topography of Vesta from Dawn FC stereo images* (pp. EPSC2012–EPSC2428). Retrieved from http://meetingorganizer.copernicus.org/EPSC2012/EPSC2012-428-1.pdf

Richardson, J., Steckloff, J., & Minton, D. (2020). Impact-produced seismic shaking and regolith growth on asteroids 433 Eros, 2867 Šteins, and 25143 Itokawa. *Icarus*, *347*, 113811. https://doi.org/10.1016/j.icarus.2020.113811

Richardson, J. E., & Abramov, O. (2020). Modeling the formation of the lunar upper megaregolith layer. *The Planetary Science Journal*, *1*(1), 2–19. https://doi.org/10.3847/psj/ab7235

Richardson, J. E., & Kedar, S. (2013). An experimental investigation of the seismic signal produced by hypervelocity impacts. *Lunar and Planetary Science Conference*, *44*, 2863.

Richardson, J. E., Melosh, H. J., & Greenberg, R. (2004). Impact-induced seismic activity on asteroid 433 Eros: A surface modification process. *Science*, *306*, 1526–1529. https://doi.org/10.1126/science.1104731

Richardson, J. E., Melosh, H. J., Greenberg, R. J., & O'Brien, D. P. (2005). The global effects of impact-induced seismic activity on fractured asteroid surface morphology. *Icarus*, *179*(2), 325–349. https://doi.org/10.1016/j.icarus.2005.07.005

Roatsch, T., Kersten, E., Matz, K.-D., Preusker, F., Scholten, F., Elgner, S., et al. (2013). High-resolution vesta low altitude mapping orbit atlas derived from dawn framing camera images. *Planetary and Space Science*, *85*, 293–298. https://doi.org/10.1016/j.pss.2013.06.024

Roberts, J. (2021). *Roberts Eros Ponds Catalog V1.1. urn:nasa:pds:ast-eros.roberts.ponds-catalog::1.1*. NASA Planetary Data System. https://doi.org/10.26033/4dqc-8067

Roberts, J. H., Kahn, E. G., Barnouin, O. S., Ernst, C. M., Prockter, L. M., & Gaskell, R. W. (2014). Origin and flatness of ponds on asteroid 433 Eros. *Meteoritics and Planetary Science*, *49*, 1735–1748. https://doi.org/10.1111/maps.12348

Robinson, M., & Carcich, B. T. (2001). *NEAR MSI DIM EROS GLOBAL BASEMAPS V1.0, NEAR-A-MSI-5-DIM-EROS/ORBIT-V1.0, NASA Planetary Data System*. Retrieved from https://arcnav.psi.edu/urn:nasa:pds:context:target:asteroid.433_eros/data

Robinson, M. S., Thomas, P. C., Veverka, J., Murchie, S., & Carcich, B. (2001). The nature of ponded deposits on Eros. *Nature*, *413*, 396–400. https://doi.org/10.1038/35096518

Robinson, M. S., Thomas, P. C., Veverka, J., Murchie, S. L., & Wilcox, B. B. (2002). The geology of 433 Eros. *Meteoritics & Planetary Sciences*, *37*, 1651–1684. https://doi.org/10.1111/j.1945-5100.2002.tb01157.x

Russell, C. T., Raymond, C. A., Coradini, A., McSween, H. Y., Zuber, M. T., Nathues, A., et al. (2012). Dawn at Vesta: Testing the protoplanetary paradigm. *Science*, *336*, 684–686. https://doi.org/10.1126/science.1219381

Saito, J., Miyamoto, H., Nakamura, R., Ishiguro, M., Michikami, T., Nakamura, A. M., et al. (2006). Detailed images of asteroid 25143 Itokawa from Hayabusa. *Science*, *312*, 1341–1344. https://doi.org/10.1126/science.1125722

Savage, R., Palafox, L., Morris, C. T., Rodriguez, J. J., Barnard, K., Byrne, S., & Hamilton, C. (2018). A Bayesian approach to subkilometer crater shape analysis using individual HiRISE images. *IEEE Transactions on Geoscience*, *56*, 1–5812. https://doi.org/10.1109/tgrs.2018.2825608

Schenk, P., Castillo-Rogez, J., Otto, K. A., O'Brien, D., Bland, M., Hughson, K., et al. (2021). Compositional control on impact crater formation on mid-sized planetary bodies: Dawn at Ceres and Vesta, Cassini at Saturn. *Icarus*, *359*, 114343. https://doi.org/10.1016/j.icarus.2021.114343

Scully, J. E. C., Poston, M., Carey, E., Baker, S., Castillo-Rogez, J., & Raymond, C. (2021). *Testing the hypothesis that curvilinear gullies, lobate deposits and pitted terrain on Vesta and ceres were formed by short-lived, debris-flow-like processes. LPSC 2021* (p. 2548). Retrieved from https://www.hou.usra.edu/meetings/lpsc2021/pdf/1252.pdf

Scully, J. E. C., Russell, C. T., Yin, A., Jaumann, R., Carey, E., Castillo-Rogez, J., et al. (2015). Geomorphological evidence for transient water flow on Vesta. *Earth and Planetary Science Letters*, *411*, 151–163. https://doi.org/10.1016/j.epsl.2014.12.004

Sears, D. W. G., Tornabene, L. L., Osinski, G. R., Hughes, S. S., & Heldmann, J. L. (2015). Formation of the "ponds" on asteroid (433) Eros by fluidization. *Planetary and Space Science*, *117*, 106–118. https://doi.org/10.1016/j.pss.2015.05.011

Sierks, H., Keller, H. U., Jaumann, R., Michalik, H., Behnke, T., Bubenhagen, F., et al. (2011). The dawn framing camera. *Space Science Reviews*, *163*, 263–327. https://doi.org/10.1007/s11214-011-9745-4

Stooke, P. (2015). *Stooke small bodies maps V3.0. MULTI-SA-MULTI-6-STOOKEMAPS-V3.0. NASA Planetary Data System*. Retrieved from https://sbn.psi.edu/pds/resource/stookemaps.html

Stopar, J., Hawke, B., Robinson, M., Denevi, B., & Giguere, T. (2012). Distribution, occurrence, and degradation of impact melt associated with small lunar craters. *Lunar and Planetary Science Conference*, 1645. Retrieved from https://www.lpi.usra.edu/meetings/lpsc2012/pdf/1645.pdf

Stopar, J. D., Hawke, B. R., Robinson, M. S., Denevi, B. W., Giguere, T. A., & Koeber, S. D. (2014). Occurrence and mechanisms of impact melt emplacement at small lunar craters. *Icarus*, *243*, 337–357. https://doi.org/10.1016/j.icarus.2014.08.011

Szalay, J. R., & Horányi, M. (2015). The search for electrostatically lofted grains above the Moon with the Lunar Dust Experiment. *Journal of Geophysical Research Letters*, *42*, 5141–5146. https://doi.org/10.1002/2015gl064324

Thomas, P. C., Prockter, L., Robinson, M., Joseph, J., & Veverka, J. (2002). Global structure of asteroid 433 Eros. *Journal of Geophysical Research Letters*, *29*, 1408–1411. https://doi.org/10.1029/2001gl014599

Thomas, P. C., & Robinson, M. S. (2005). Seismic resurfacing by a single impact on the asteroid 433 Eros. *Nature*, *436*, 366–369. https://doi.org/10.1038/nature03855

Veverka, J., Robinson, M., Thomas, P., Murchie, S., Bell, J. F., Izenberg, N., et al. (2000). NEAR at Eros: Imaging and spectral results. *Science*, *289*, 2088–2097. https://doi.org/10.1126/science.289.5487.2088

Veverka, J., Thomas, P. C., Robinson, M., Murchie, S., Chapman, C., Bell, M., et al. (2001). Imaging of small-scale features on 433 Eros from NEAR: Evidence for a complex regolith. *Science*, *292*, 484–488. https://doi.org/10.1126/science.1058651

Williams, D. A., Denevi, B. W., Mittlefehldt, D. W., Mest, S. C., Schenk, P. M., Yingst, R. A., et al. (2014). The geology of the Marcia quadrangle of asteroid Vesta: Assessing the effects of large, young craters. *Icarus*, *244*, 74–88. https://doi.org/10.1016/j.icarus.2014.01.033

Williams, D. A., O'Brien, D. P., Schenk, P. M., Denevi, B. W., Carsenty, U., Marchi, S., et al. (2014). Lobate and flow-like features on asteroid Vesta. *Planetary and Space Science*, *103*, 24–35. https://doi.org/10.1016/j.pss.2013.06.017

Yano, H., Kubota, T., Miyamoto, H., Okada, T., Scheeres, D., Takagi, Y., et al. (2006). Touchdown of the Hayabusa spacecraft at the muses sea on Itokawa. *Science*, *312*, 1350–1353. https://doi.org/10.1126/science.1126164